Optical Coherence Tomography Angiography in Glaucoma

Dr. Shruthi Srinivasaiah, Dr. Zia Pradhan, Dr. Narendra Puttaiah, Dr. Harsha Rao

Narayana Nethralaya, Bengaluru, India

PATHOGENESIS OF GLAUCOMA

Glaucoma is a chronic optic neuropathy characterised by progressive loss of retinal ganglion cells (RGCs)[1]. Although the exact pathogenesis of glaucoma is not fully understood, two main theories have been proposed to explain the death of RGCs in glaucoma[2]. The "mechanical theory" postulates RGC death to be a consequence of raised intraocular pressure (IOP). It proposes that increased IOP causes an obstruction to the axoplasmic flow within the RGCs at the lamina cribrosa leading to RGC death[3]. Multiple studies have reported IOP to be a major causal factor for glaucoma, with the risk of incident glaucoma and its progression increasing with higher IOP[4-10]. However, it is well accepted that the mechanical theory alone, fails to explain the entire pathogenic mechanism of glaucoma. This is because glaucoma occurs and progresses even at normal IOP levels in a significant number of eyes, and not all eyes with ocular hypertension develop glaucoma. The "vascular theory", the alternate theory to explain glaucoma pathogenesis, proposes reduced blood supply to the RGCs, as the primary cause of glaucoma[11-13].

OCULAR BLOOD SUPPLY: ANATOMY AND PHYSIOLOGY

Ocular blood supply occurs predominantly through the retinal and the choroidal circulations which are both derived from the ophthalmic artery. The inner one-third of the retina is supplied by the central retinal artery (retinal circulation) while the outer two-thirds of the retina is supplied by branches of the choroidal vessels (choroidal circulation). Similarly, the superficial layer of the optic nerve head (ONH) which comprises of the RGC axons receives its blood supply via small branches of the central retinal artery. The deeper tissues of the ONH, such as the prelaminar region, are supplied by branches from recurrent choroid arterioles and the short posterior ciliary arteries[14,15]. The venous drainage of the entire ONH is via the central retinal vein.

The physiology of ocular blood flow has been enumerated in previous studies[16,17]. Retinal circulation is a low flow, high oxygen extraction system with no autonomic innervation. The presence of endothelial tight junctions results in a blood–retinal barrier, similar to the blood–brain barrier. Retinal circulation has autoregulation so that the blood flow is held fairly constant in spite of mild to moderate changes in the perfusion pressure and IOP. In contrast, choroidal circulation is a high flow, low oxygen extraction system. Choroid has a rich autonomic innervation and the endothelium of the choroidal vessels are fenestrated. The choroidal circulation has poor autoregulation, which renders the choroidal blood flow more dependent on perfusion pressure.

MEASURING OCULAR BLOOD FLOW IN HUMANS

Retinal and ONH blood flow in glaucomatous eyes has been investigated earlier using various techniques. Fluorescein angiography (FA), a common technique used to evaluate retinal vasculopathies, has been used to study ocular blood flow in glaucoma. The studies using FA have reported prolonged arteriovenous passage times[18,19] fluorescein filling defects in the disc[20,21] focal sector hypoperfusion of the optic disc and diffuse disc hypo-perfusion[22] in patients with glaucoma. However, FA is an invasive technique requiring the intravenous injection of a dye, and the transient presence of the dye in the eye makes quantification difficult.

Laser Doppler flowmetry (LDF) and laser speckle flowgraphy (LSFG) are two other non-invasive techniques that have been used to measure ONH perfusion. Multiple studies with these two techniques have reported significantly reduced neuroretinal rim (NRR) blood flow and peripapillary retinal blood flow in patients with glaucoma compared to controls[23-27]. However, measurements provided by LDF and LSFG are too variable for diagnostic application. Coefficient of variation (CV) for intra-visit repeatability with LDF has been reported to range from 6.6% to 21.2% and for inter-visit reproducibility from 25.2% to 30.1%[28-32]. With LSFG, CVs for intra-visit repeatability have been reported to range from 1.9% to 11.9%, and inter-visit reproducibility was 12.8%[33-35].

The search for a simple, non-invasive, reproducible method of evaluating the ocular blood flow lead to the development of optical coherence tomography (OCT) angiography.

OCT ANGIOGRAPHY

A number of techniques using OCT have been developed for imaging the ocular blood flow. Doppler OCT was one of the earliest techniques developed for vascular imaging. It assessed blood flow by comparing phase differences between adjacent A-scans[36]. Although Doppler OCT was appropriate for large vessels around the disc, it was not sensitive enough to measure accurately the low velocities in small vessels that make up the ONH and retinal microcirculation.

The current OCT angiography (OCTA) technology is capable of imaging large vessels as well as microvasculature of the retina and ONH by performing multiple OCT scans of the same region. The variation in OCT signal at each location is then studied since moving particles, such as red blood cells, result in

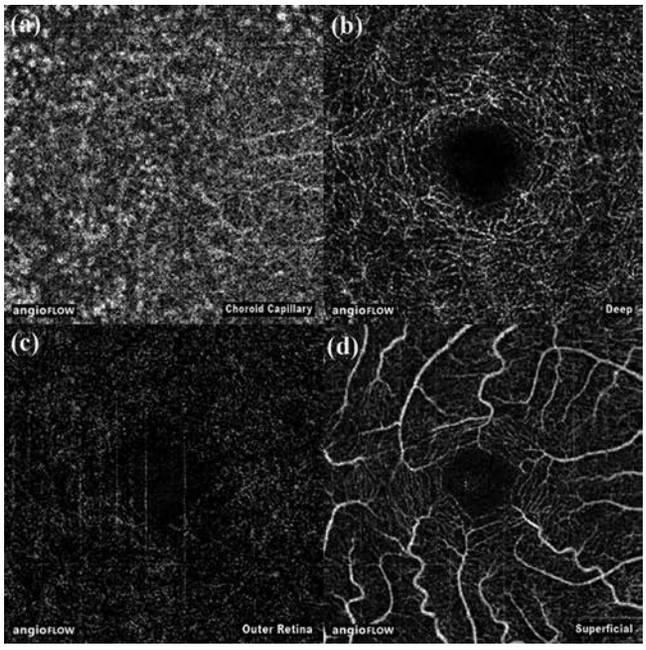

Figure 1: *Angiography slabs of the macular scan obtained using spectral domain optical coherence tomography showing the choriocapillaris (a), deep retinal (b), outer retinal (c) and superficial retinal (d) slabs.*

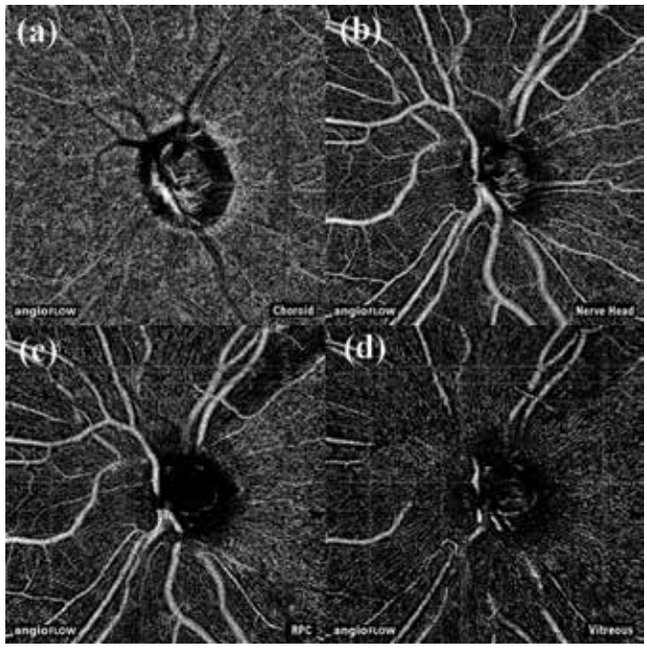

Figure 2: *Angiography slabs of the optic nerve head scan obtained using spectral domain optical coherence tomography showing the choroid (a), nerve head (b), radial peripapillary capillary, RPC (c) and vitreous (d) slabs.*

a high variance of the OCT signal between scans and this is used to identify blood vessels. There are several algorithms which have been developed to interpret the OCT signals to delineate the blood vessels. The split spectrum amplitude decorrelation angiography (SSADA) uses the variation in the intensity of the OCT signal to identify blood vessels. The fluctuating value of OCT intensities is considered as the decorrelation (D). Thus, pixels in the B-scan frame where blood is flowing have fluctuating intensities and yield high D values (approaching 1). Pixels in the B-scan frames that contain static tissue yield small D values (approaching 0)[37]. The principles of SSADA have been explained in detail by Jia et al.[38] The optical microangiography (OMAG), another algorithm that performs OCTA (Angioplex, Cirrus HD-OCT, Carl Zeiss Meditec Inc., Dublin, CA), uses the variation in intensity as well as the phase difference of the OCT signals for vessel delineation. In addition to tracing the blood vessels, these algorithms also strive to reduce motion artefacts and pulsatile bulk motion noise.

Two other developments that improved OCTA technology were the en face presentation and motion correction. En face presentation helps to reduce the data complexity by presenting angiography information in 2 dimensions. Retina is segmented into different slabs, such as choriocapillaris, outer and deep retina and superficial retina, and vessels in each of these slabs is presented in 2-dimensional format (Figure 1). ONH is similarly segmented into choroid, nerve head, radial peripapillary capillary and vitreous slabs (Figure 2). As the time required to obtain the scan with OCTA is close to 3 seconds, involuntary saccades and changes in fixation during data acquisition can lead to motion artifacts that may confound the interpretation of the final OCT angiogram. "Motion Correction Technology" (MCT) is an orthogonal registration algorithm which minimizes these motion artifacts[39].

SSADA has been optimized for the spectral-domain OCT (SDOCT) platform[40]. This algorithm is currently available on a commercial OCT device (RTVue-XR SD-OCT, Optovue Inc., Fremont, CA) making the OCTA technology available to clinicians. This review focusses only on OCTA performed using the SSADA algorithm.

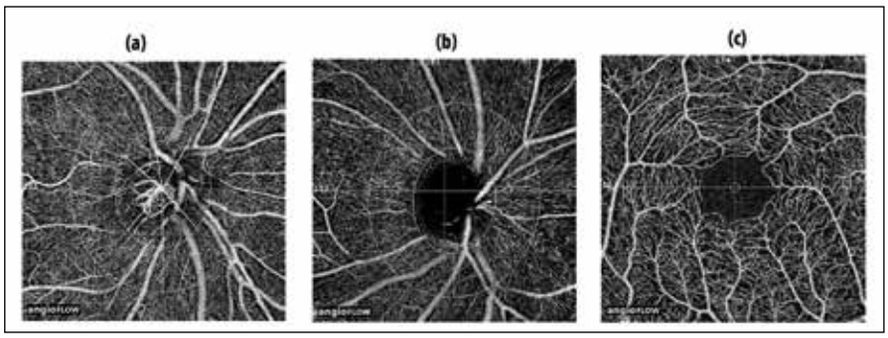

Figure 3: *Figure showing the optic nerve head (a), peripapillary (b), and macular (c) optical coherence tomography angiography images and the sectors where vessel densities are calculated. The optic disc vessel density is calculated within the optic nerve head from the nerve head segment of the en face angiogram, peripapillary vessel density over a 0.75 mm-wide elliptical annulus extending from the optic disc boundary from the radial peripapillary capillary segment, and superficial macular vessel density over a 1.5 mm-wide circular annulus centered on the macula.*

INTERPRETING THE OCTA PRINT-OUT OF A NORMAL EYE

The current generation of OCTA can scan the optic disc region and the macula. The optic disc OCTA scan is performed using volumetric scans covering an area of 4.5 × 4.5 mm and the software automatically fits an ellipse to the optic disc margin. The region within this margin is referred to as the "inside disc' region (Figure 3a). The peripapillary region is defined as a 0.75 mm-wide elliptical annulus extending from the optic disc boundary (Figure 3b). This region may be divided in 6 sectors based on the Garway-Heath map or into 8 peripapillary sectors similar to that of the

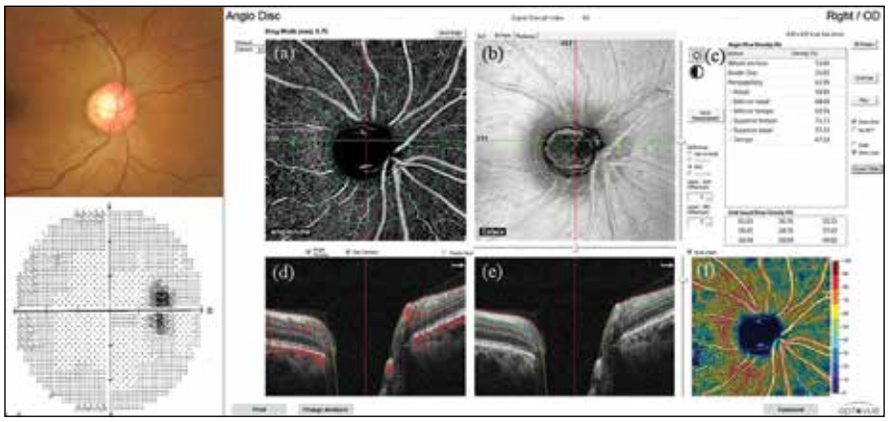

Figure 4: *Peripapillary OCTA report of an eye showing normal optic disc (upper left) and normal visual fields (lower left). The OCTA report shows dense radial peripapillary capillaries on the angiography image (a) and heat map (f) with vessel densities in different sectors quantified in the table (c).*

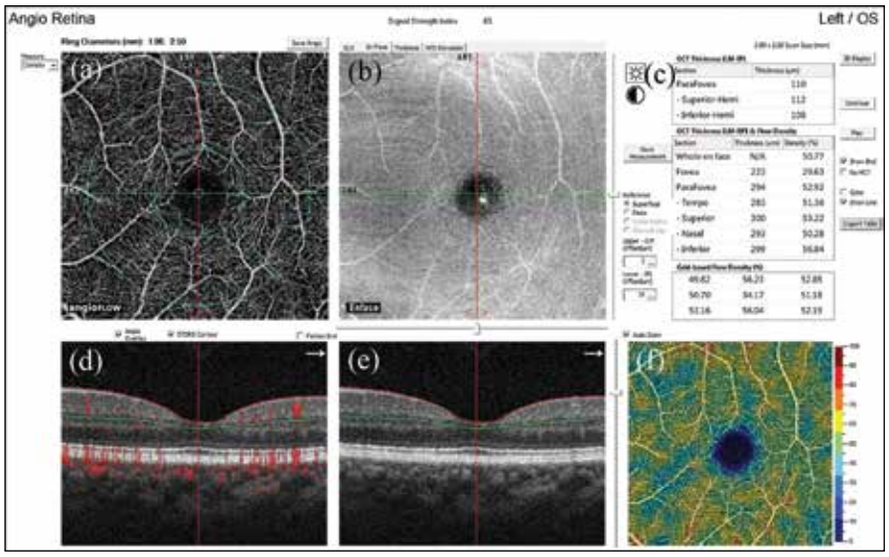

Figure 5: *Macular OCTA report showing the superficial retinal vessels of a normal eye. The OCTA report shows dense capillaries on the angiography image (a) and heat map (f) with vessel densities in different sectors quantified in the table (c).*

RNFL maps (temporal-upper TU, supero-temporal ST, supero-nasal SN, nasal-upper NU, nasal-lower NL, infero-nasal IN, infero-temporal IT and temporal-lower TL). The optic disc scan can be divided into several slabs for further analysis. The most superficial "vitreous" slab is usually used for assessing neovascularization of the disc and is not used in glaucoma. The "nerve head" layer extends from the internal limiting membrane (ILM) to 150 microns posterior and is used for assessing the vasculature within the optic disc. The "radial peripapillary capillary (RPC)" layer extends from the ILM to the posterior boundary of the RNFL and is used for assessing the vascular supply of the RNFL layer of the peripapillary region. And the "choroidal slab" is used to assess the deep retinal and choroidal vasculature.

The macular OCTA scan is performed using a volumetric scan covering a 3 x 3 mm area (Figure 3c). More recently 6 x 6 mm scans of the macula are also available. The macular region is divided in the small central foveal area and a 1.5 mm wide parafoveal, circular annulus. This parafoveal region is divided in 2 hemispheres of 180 degrees each (superior and inferior). Additionally, it may also be divided into 4 sectors of 90 degrees each (nasal, inferior, superior, and temporal sectors). The macular region is also divided into slabs for further analysis. The superficial retinal slab extends from 3 µm below the ILM to 15 µm below the inner plexiform layer (IPL). Deep retinal slab extends from 15 µm below IPL to 70 µm below the IPL. Outer retinal slab extends from 70 µm below the IPL to 30 µm below the retinal pigment epithelium (RPE) and choroid capillary slab extends from 30 µm below the RPE to 60 µm below the RPE.

OCTA quantifies the ocular circulation using two parameters: flow index and vessel density. Flow index is defined as the average decorrelation values in the measured area, and vessel density, which is the most widely used OCTA parameter, is defined as the percentage area occupied by vessels in the measured area. The threshold decorrelation value used to separate blood vessel and static tissue is set at 0.125, which is two standard deviations above the mean decorrelation value in the foveal avascular zone, a region devoid of vessels. Quantification of vessel density can be performed in the nerve head and the RPC slab of the optic disc scan, but not the choroidal slab. Similarly, vessel densities can also be determined for the superficial vascular plexus of the macula scan. The current OCTA machines do not contain a normative database for comparison of the patient's vessel densities. Currently these comparisons are made in research studies using control eyes.

Figure 4 shows the peripapillary OCTA report of a normal eye (showing normal optic disc and visual field). The OCTA report shows

(Figure 4a) angiography image showing large vessels and a dense network of capillaries in the RPC segment

(Figure 4b) En face image

(Figure 4d and e) B scan showing the segmentation lines (for the RPC segment) along with the blood vessels detected by the SSADA algorithm

(Figure 4f) Heat map showing dense network of vessels in the peripapillary region; represented by warm colors such as red and yellow

(Figure 4c) Table showing the vessel density in the entire scan region and various sectors

Figure 5 shows a macular OCTA report of a normal eye showing the superficial retinal vessels. Macular scan is performed using a 3 mm x 3 mm scan. The interpretation of the report is similar to that of the peripapillary report described earlier.

Interpreting the OCTA print-out of a glaucomatous eye: A qualitative analysis

Figure 6 shows a glaucomatous eye (mild severity of disease) with a superior neuroretinal rim notch and superotemporal RNFL defect (indicated by arrows on the disc photograph) with a correlating inferior hemifield defect on the visual fields. OCTA shows reduced vessel density in the superotemporal region on the angiography and the heat

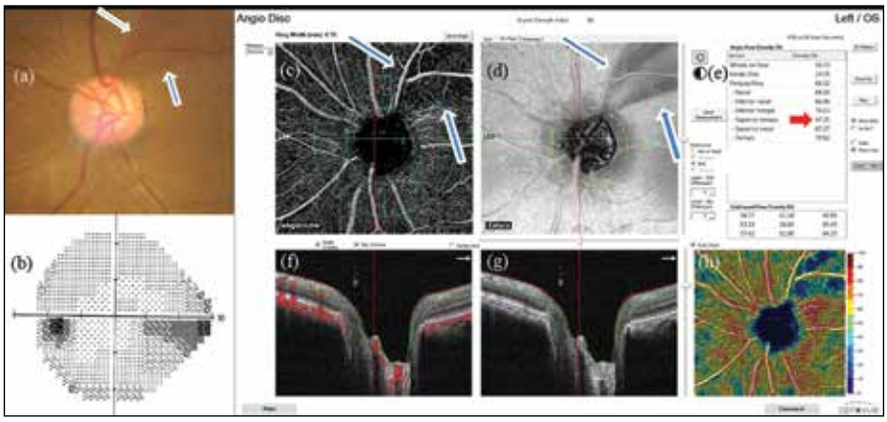

Figure 6: *Peripapillary OCTA report of a glaucomatous eyes with mild disease. Optic disc photograph (a) shows superior neuroretinal rim notch and superotemporal RNFL defect (indicated by arrows on the disc photograph) with a correlating inferior hemifield defect on the visual fields (b). OCTA report shows reduced vessel density in the superotemporal region as indicated by the arrows on the angiography (c) and heat map (h), along with a decrease in the vessel density in the corresponding region on the table (e, red arrow).*

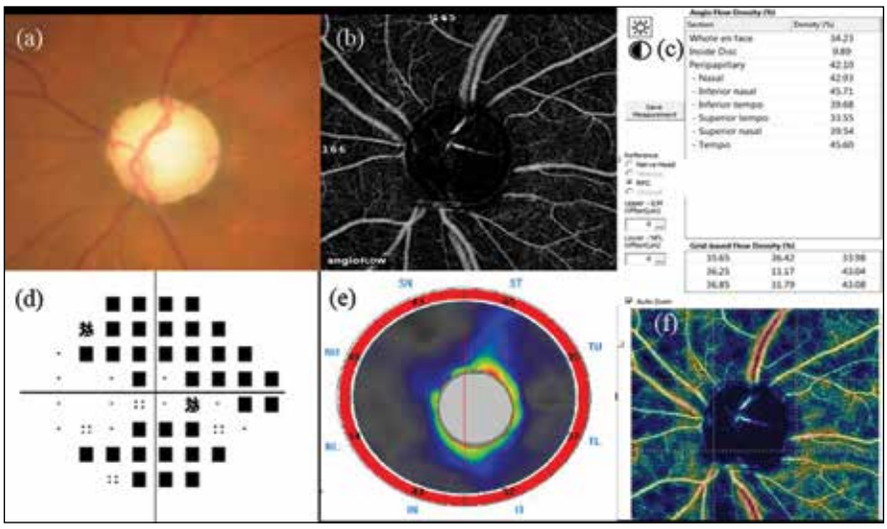

Figure 7: *Peripapillary OCTA report of a glaucomatous eyes with advanced disease. It shows advanced disc damage (a), bi-arcuate visual field loss (b) and diffuse RNFL thinning (e). OCTA report shows gross loss of capillaries on the angiography (b) and heat map (f), along with a decrease in the vessel densities in all peripapillary OCTA sectors in the table (c).*

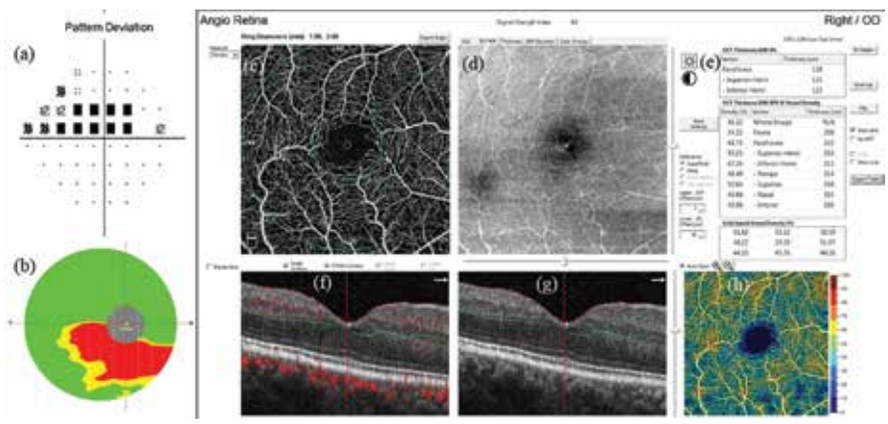

Figure 8: *Macular OCTA report of a glaucomatous eye which shows a superior hemifield defect (a) and a corresponding inferior ganglion cell complex thinning (b). OCTA shows reduced superficial macular vessel density in the inferior region better noted on the heat map (h) and quantified in the table (e).*

map, along with a decrease in the vessel density in the corresponding sector.

Figure 7 shows an eye with advanced glaucoma. OCTA shows gross loss of capillaries on the angiography and heat map, along with a decrease in the vessel densities in all peripapillary sectors in the Table.

Figure 8 shows a glaucomatous eye with superior hemifield defect and a corresponding inferior ganglion cell complex (GCC) thinning. OCTA shows reduced superficial retinal vessel density in the inferior macular region noted on the heat map. Figure 9 shows the heat map of macular OCTA scan of the same eye performed with 6 mm x 6 mm scan. Compared to the 3 mm x 3 mm scan, the vessel dropouts are more obvious on the 6 mm x 6 mm scan.

A quantitative analysis of OCTA changes in different subtypes of glaucoma

(i) POAG: All the initial studies with OCTA were performed in eyes with primary open angle glaucoma (POAG) and showed reduced flow index and vessel density inside the ONH and in the peripapillary region of eyes with POAG compared to controls[41-43]. Multiple studies subsequently showed that the OCTA vessel densities measured in the macular regions were also reduced in eyes with glaucoma compared to control eyes[44,45]. Peripapillary vessel density reduction was found to be significantly greater than that inside the ONH and the macular region in glaucomatous eyes.

(ii) Normal tension glaucoma: Vascular theory of glaucoma is considered to be more applicable in eyes developing glaucomatous damage at low IOP. A few studies compared the OCTA measurements in low pressure glaucoma (NTG) and high pressure glaucoma (POAG). However, no difference in OCTA measurements were seen between NTG and severity-matched POAG eyes[46].

(iii) Angle closure glaucoma: OCTA measurements in primary angle closure glaucoma (PACG) were found to be similar to that in POAG when the severity of disease was matched for[47] Like POAG (described below), OCT neuronal (NRR, RNFL and GCC) measurements had a better diagnostic ability compared to OCTA vessel density measurements (inside ONH, in peripapillary and macular regions) in PACG[48].

(iv) Pseudoexfoliation glaucoma: A few studies have evaluated the superficial retinal vasculature in the peripapillary region of PXG eyes and have reported that the reduction of vessel densities was greater in PXG compared to POAG eyes of similar disease severity[49, 50].

OCTA CHANGES IN PERIMETRICALLY INTACT REGIONS OF GLAUCOMATOUS EYES

It is important to determine the

temporal relationship of vessel density reduction on OCTA with respect to RNFL thinning and visual field defects. This would help us develop strategies to detect the disease in the earliest stages. A longitudinal study is required to address this question. However, OCTA is a relatively new technology and there are, currently, no longitudinal studies addressing this question. As an alternate approach, studies have been performed in eyes with established perimetric glaucoma, whose visual field defects are limited to one hemifield; and the vascular changes in regions corresponding to the intact hemifield have been examined. These studies have found reduced peripapillary vessel density and RNFL thickness in the hemiretina corresponding to the perimetrically intact hemifield compared to that of healthy eyes[51-53]. One of these studies also found that the temporal sector of the perimetrically intact hemifield (corresponding to the region of papillomacular bundles) showed reduced vessel density in the presence of normal RNFL thickness. This suggested that there may be regional variations in the alterations of RNFL thickness and vessel density measurements, and OCTA changes may precede RNFL changes in some sectors.

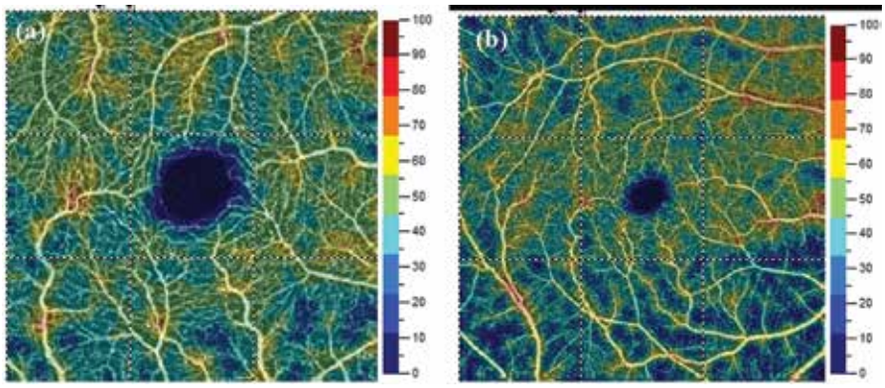

Figure 9: *Macular OCTA report of the eye shown in Figure 8 imaged using a 3 mm x 3 mm (a) and a 6 mm x 6 mm scan (b). Compared to the 3 mm x 3 mm scan, the vessel dropouts are more obvious on the 6 mm x 6 mm scan.*

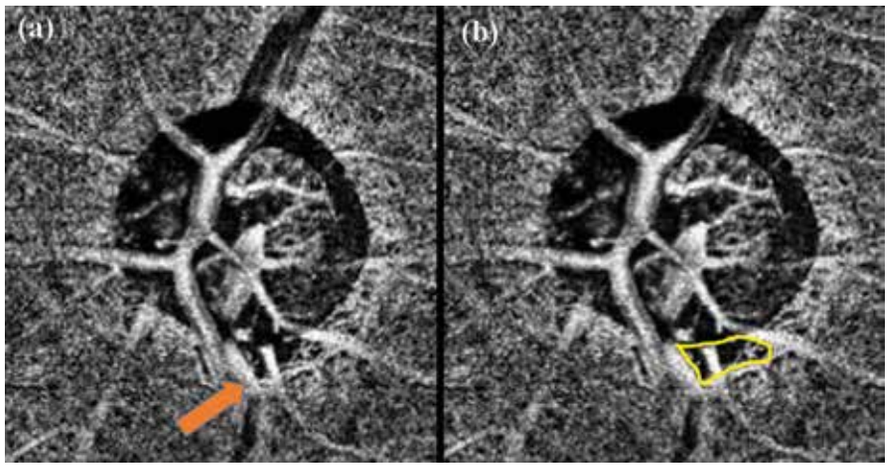

Figure 10: *Choroidal OCTA slab of a glaucomatous eye showing the presence of choroidal microvasculature dropout (CMvD) in the inferior region (a). Arrow points to the CMvD. Yellow line marks out the boundary of the CMvD (b).*

COMPARING OCTA WITH OCT MEASUREMENTS IN DIAGNOSING GLAUCOMA

A number of studies have compared the diagnostic abilities of OCTA measurements (vessel densities of the inside disc, peripapillary and macular regions) with corresponding OCT measurements (ONH neuroretinal rim area, RNFL and macular thickness) in glaucoma.

A few studies comparing the diagnostic abilities (area under the receiver operating characteristic curves [AUC] and sensitivities at high specificities) of peripapillary vessel densities and RNFL thickness in POAG have found them to similar. Depending on the severity of glaucoma patients included in these studies, the AUCs of both peripapillary vessel density and RNFL thickness have ranged between 0.85 to 0.95. A few other studies have reported a better diagnostic ability of RNFL thickness compared to peripapillary vessel density in POAG[54]. In spite of the AUCs being similar, one study showed that the sensitivity to detect glaucoma in early stages of severity was better with RNFL thickness compared to peripapillary vessel density measurements. Diagnostic abilities of vessel density measurements inside ONH were found to be significantly lesser than that of the OCT measured NRR area. Similar to the peripapillary measurements, diagnostic ability of superficial retinal vessel density at macula was found to be similar to that of macular GCC thickness by one study[55] while the same was found to be inferior to GCC thickness by another study. However, macular vessel densities in all these studies were evaluated on 3 mm x 3 mm scans, and a subsequent study showed that evaluating the macular vessel densities on 6 mm x 6 mm scans would be able to better detect glaucomatous changes[56]. It is still not clear if OCTA measured vessel density changes occur before or after OCT measured neuronal (NRR, RNFL and GCC) changes in glaucoma. Longitudinal studies in the future should be able to clarify this.

OCTA OF THE PERIPAPILLARY CHOROID

Peripapillary choroidal circulation is of particular interest in glaucoma as it may be a surrogate marker for the perfusion of the deep ONH structures. Recently, choroidal microvasculature dropout (CMvD, Figure 10), defined as the complete loss of choriocapillaris in localized regions of parapapillary atrophy (PPA), has been observed using OCTA in POAG eyes[57,58]. CMvD has been shown to be a true perfusion defect using indocyanine green angiography[59]. Studies have also reported a topographic association between the location of CMvD and structural defects (RNFL thinning and lamina cribrosa defects) as well as functional defects (visual field loss) in POAG eyes[60,61]. CMvD is a relatively novel finding in glaucoma and the clinical implications of it are not fully known. It has been argued that CMvD is likely to precede glaucomatous ONH damage[62]. A recent study reported an association between CMvD and progressive RNFL thinning in POAG eyes with DH[63]. Longitudinal studies are required to determine the clinical implication of CMvD in glaucoma.

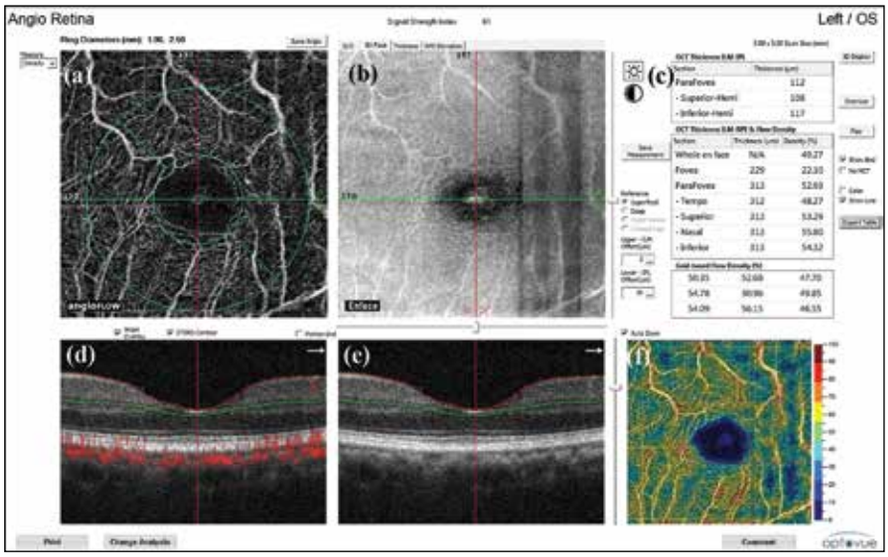

Figure 11: *Macular OCTA scan showing two types of artifacts; motion artifacts, recognized as vertical bands temporally on the en face map (b) and duplication of vessels, recognized inferiorly and nasally on the angiography map (a). These artifacts cause a decrease in vessel density in the temporal sector and increase in vessel density in the nasal and inferior sectors (noted on the heat map [f] and table [c]).*

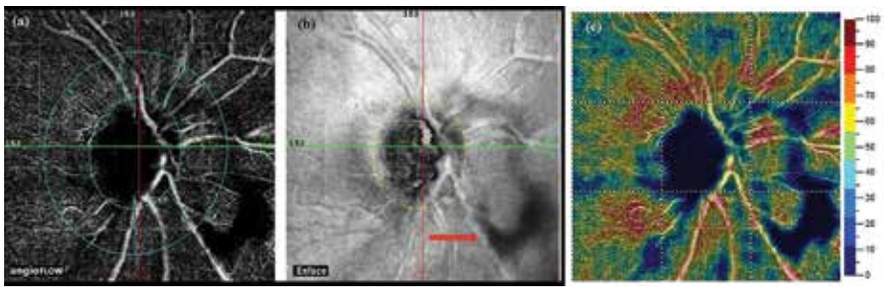

Figure 12: *Vitreous opacity (red arrow on en face map [b]) casting a shadow, as seen on the angiography map (a) and causing a falsely reduced vessel density on the heat map (c).*

FACTORS AFFECTING OCTA MEASUREMENTS

Unlike the neuronal elements, vasculature is affected by multiple factors other than glaucoma. A study evaluated the effect of subject-related (age, gender, systemic hypertension and diabetes), eye-related (refractive error, optic disc size) and technology-related (signal strength index, SSI of the scans) determinants on the peripapillary and macular vessel densities in normal eyes[64]. It found that peripapillary vessel densities were higher in females. Peripapillary vessel densities were lower, while the macular vessel density was higher, in subjects with hypertension. Most of the vessel densities were lower in subjects with diabetes. In addition to these factors, SSI of the OCTA scans showed a significant positive association with the vessel densities of all regions. Vessel densities were higher in scans with higher SSI values. These results should be considered while interpreting the vessel densities in glaucoma.

LIMITATIONS AND RECENT ADVANCES IN OCTA

Motion artifacts are common with OCTA imaging due to the prolonged time required to acquire the scans; in spite of methods available to account for the artifacts (Figure 11). This is true even in research settings and multiple studies have also reported high number of poor quality images with OCTA[65-68]. Two significant improvements incorporated recently to overcome the issue of poor quality scans are (i) real time eye tracking technology, for controlling the motion artifacts more effectively[69] and, (ii) high-density (HD) scanning mode, for improving the resolution of the scans. A recent study has reported that the number of poor quality scans significantly decreased with the incorporation of these improvements[70].

Media opacities, especially vitreous opacities, can significantly affect the quality of OCTA scans and the quantification of vessel densities (Figure 12).

OCTA technology is able to evaluate the superficial retinal vessels well but not the deeper retinal and choroidal vasculature. This is because the signals from the superficial retinal vessels project on to the deeper layers causing artifacts known as the projection artifacts. Detection of CMvD, for example, is affected by the presence of projection artifacts. Newer methods of projection artifact correction have been tried and the newer generations of OCTA (projection resolved OCTA) are likely to evaluate the deeper retinal and choroidal vasculature better[71].

CONCLUSIONS

OCTA has the potential to be useful in the diagnosis and monitoring of glaucoma. However, the technology needs to mature before it becomes a routine part of the glaucoma work-up in our clinics.

REFERENCES

1. Weinreb RN, Aung T, Medeiros FA. The pathophysiology and treatment of glaucoma: a review. JAMA 2014;311:1901-11.
2. Fechtner RD, Weinreb RN. Mechanisms of optic nerve damage in primary open angle glaucoma. Surv Ophthalmol 1994;39:23-42.
3. Yan DB, Coloma FM, Metheetrairut A, et al. Deformation of the lamina cribrosa by elevated intraocular pressure. Br J Ophthalmol 1994;78:643-8.
4. Francis BA, Varma R, Chopra V, et al. Intraocular pressure, central corneal thickness, and prevalence of open-angle glaucoma: the Los Angeles Latino Eye Study. Am J Ophthalmol 2008;146:741-6.
5. Sommer A, Tielsch JM, Katz J, et al. Relationship between intraocular pressure and primary open angle glaucoma among white and black Americans. The Baltimore Eye Survey. Arch Ophthalmol 1991;109:1090-5.
6. The Advanced Glaucoma Intervention Study (AGIS): 7. The relationship between control of intraocular pressure and visual field deterioration.The AGIS Investigators. Am J Ophthalmol 2000;130:429-40.
7. Lichter PR, Musch DC, Gillespie BW, et al. Interim clinical outcomes in the Collaborative Initial Glaucoma Treatment Study comparing initial treatment randomized to medications or surgery. Ophthalmology 2001;108:1943-53.
8. Kass MA, Heuer DK, Higginbotham EJ, et al. The Ocular Hypertension Treatment Study: a randomized trial determines that topical ocular hypotensive medication delays or prevents the onset of primary open-angle glaucoma.

Arch Ophthalmol 2002;120:701-13; discussion 829-30.
9. Leske MC, Heijl A, Hussein M, et al. Factors for glaucoma progression and the effect of treatment: the early manifest glaucoma trial. Arch Ophthalmol 2003;121:48-56.
10. Ernest PJ, Schouten JS, Beckers HJ, et al. An evidence-based review of prognostic factors for glaucomatous visual field progression. Ophthalmology 2013;120:512-9.
11. Flammer J. The vascular concept of glaucoma. Surv Ophthalmol 1994;38 Suppl:S3-6.
12. Bonomi L, Marchini G, Marraffa M, et al. Vascular risk factors for primary open angle glaucoma: the Egna-Neumarkt Study. Ophthalmology 2000;107:1287-93.
13. Leske MC, Heijl A, Hyman L, et al. Predictors of long-term progression in the early manifest glaucoma trial. Ophthalmology 2007;114:1965-72.
14. Hayreh SS. Blood supply of the optic nerve head. Ophthalmologica 1996;210:285-95.
15. Hayreh SS. The blood supply of the optic nerve head and the evaluation of it - myth and reality. Prog Retin Eye Res 2001;20:563-93.
16. Bill A, Nilsson SF. Control of ocular blood flow. J Cardiovasc Pharmacol 1985;7 Suppl 3:S96-102.
17. Flammer J, Orgul S. Optic nerve blood-flow abnormalities in glaucoma. Prog Retin Eye Res 1998;17:267-89.
18. Arend O, Plange N, Sponsel WE, Remky A. Pathogenetic aspects of the glaucomatous optic neuropathy: fluorescein angiographic findings in patients with primary open angle glaucoma. Brain Res Bull 2004;62:517-24.
19. Huber K, Plange N, Remky A, Arend O. Comparison of colour Doppler imaging and retinal scanning laser fluorescein angiography in healthy volunteers and normal pressure glaucoma patients. Acta Ophthalmol Scand 2004;82:426-31.
20. Talusan E, Schwartz B. Specificity of fluorescein angiographic defects of the optic disc in glaucoma. Arch Ophthalmol 1977;95:2166-75.
21. Schwartz B, Rieser JC, Fishbein SL. Fluorescein angiographic defects of the optic disc in glaucoma. Arch Ophthalmol 1977;95:1961-74.
22. Hitchings RA, Spaeth GL. Fluorescein angiography in chronic simple and low-tension glaucoma. Br J Ophthalmol 1977;61:126-32.
23. Piltz-seymour JR, Grunwald JE, Hariprasad SM, Dupont J. Optic nerve blood flow is diminished in eyes of primary open-angle glaucoma suspects. Am J Ophthalmol 2001;132:63-9.
24. Hamard P, Hamard H, Dufaux J, Quesnot S. Optic nerve head blood flow using a laser Doppler velocimeter and haemorheology in primary open angle glaucoma and normal pressure glaucoma. Br J Ophthalmol 1994;78:449-53.
25. Michelson G, Langhans MJ, Groh MJ. Perfusion of the juxtapapillary retina and the neuroretinal rim area in primary open angle glaucoma. J Glaucoma 1996;5:91-8.
26. Hafez AS, Bizzarro RL, Lesk MR. Evaluation of optic nerve head and peripapillary retinal blood flow in glaucoma patients, ocular hypertensives, and normal subjects. Am J Ophthalmol 2003;136:1022-31.
27. Yokoyama Y, Aizawa N, Chiba N, et al. Significant correlations between optic nerve head microcirculation and visual field defects and nerve fiber layer loss in glaucoma patients with myopic glaucomatous disk. Clin Ophthalmol 2011;5:1721-7.
28. Yaoeda K, Shirakashi M, Funaki S, et al. Measurement of microcirculation in the optic nerve head by laser speckle flowgraphy and scanning laser Doppler flowmetry. Am J Ophthalmol 2000;129:734-9.
29. Kagemann L, Harris A, Chung HS, et al. Heidelberg retinal flowmetry: factors affecting blood flow measurement. Br J Ophthalmol 1998;82:131-6.
30. Luksch A, Lasta M, Polak K, et al. Twelve-hour reproducibility of retinal and optic nerve blood flow parameters in healthy individuals. Acta Ophthalmol 2009;87:875-80.
31. Nicolela MT, Hnik P, Schulzer M, Drance SM. Reproducibility of retinal and optic nerve head blood flow measurements with scanning laser Doppler flowmetry. J Glaucoma 1997;6:157-64.
32. Iester M, Altieri M, Michelson G, et al. Intraobserver reproducibility of a two-dimensional mapping of the optic nerve head perfusion. J Glaucoma 2002;11:488-92.
33. Aizawa N, Yokoyama Y, Chiba N, et al. Reproducibility of retinal circulation measurements obtained using laser speckle flowgraphy-NAVI in patients with glaucoma. Clin Ophthalmol 2011;5:1171-6.
34. Yaoeda K, Shirakashi M, Funaki S, et al. Measurement of microcirculation in optic nerve head by laser speckle flowgraphy in normal volunteers. Am J Ophthalmol 2000;130:606-10.
35. Tamaki Y, Araie M, Tomita K, et al. Real-time measurement of human optic nerve head and choroid circulation, using the laser speckle phenomenon. Jpn J Ophthalmol 1997;41:49-54.
36. Wang Y, Bower BA, Izatt JA, et al. Retinal blood flow measurement by circumpapillary Fourier domain Doppler optical coherence tomography. J Biomed Opt 2008;13:064003.
37. Jia Y, Morrison JC, Tokayer J, et al. Quantitative OCT angiography of optic nerve head blood flow. Biomed Opt Express 2012;3:3127-37.
38. Jia Y, Tan O, Tokayer J, et al. Split-spectrum amplitude-decorrelation angiography with optical coherence tomography. Opt Express 2012;20:4710-25.
39. Kraus MF, Potsaid B, Mayer MA, et al. Motion correction in optical coherence tomography volumes on a per A-scan basis using orthogonal scan patterns. Biomed Opt Express 2012;3:1182-99.
40. Gao SS, Liu G, Huang D, Jia Y. Optimization of the split-spectrum amplitude-decorrelation angiography algorithm on a spectral optical coherence tomography system. Opt Lett 2015;40:2305-8.
41. Jia Y, Wei E, Wang X, et al. Optical coherence tomography angiography of optic disc perfusion in glaucoma. Ophthalmology 2014;121:1322-32.
42. Liu L, Jia Y, Takusagawa HL, et al. Optical Coherence Tomography Angiography of the Peripapillary Retina in Glaucoma. JAMA Ophthalmol 2015;133:1045-52.
43. Yarmohammadi A, Zangwill LM, Diniz-Filho A, et al. Optical Coherence Tomography Angiography Vessel Density in Healthy, Glaucoma Suspect, and Glaucoma Eyes. Invest Ophthalmol Vis Sci 2016;57:OCT451-9.
44. Rao HL, Pradhan ZS, Weinreb RN, et al. Regional Comparisons of Optical Coherence Tomography Angiography Vessel Density in Primary Open-Angle Glaucoma. Am J Ophthalmol 2016;171:75-83.
45. Rao HL, Pradhan ZS, Weinreb RN, et al. A comparison of the diagnostic ability of vessel density and structural measurements of optical coherence tomography in primary open angle glaucoma. PLoS One 2017;12:e0173930.
46. Scripsema NK, Garcia PM, Bavier RD, et al. Optical Coherence Tomography Angiography Analysis of Perfused Peripapillary Capillaries in Primary Open-Angle Glaucoma and Normal-Tension Glaucoma. Invest Ophthalmol Vis Sci 2016;57:OCT611-OCT20.
47. Rao HL, Kadambi SV, Weinreb RN, et al. Diagnostic ability of peripapillary vessel density measurements of optical coherence tomography angiography in primary open-angle and angle-closure glaucoma. Br J Ophthalmol 2017;101:1066-70.
48. Rao HL, Pradhan ZS, Weinreb RN, et al. Vessel Density and Structural Measurements of Optical Coherence Tomography in Primary Angle Closure and Primary Angle Closure Glaucoma. Am J Ophthalmol 2017;177:106-15.
49. Suwan Y, Geyman LS, Fard MA, et al. Peripapillary Perfused Capillary Density in Exfoliation Syndrome and Exfoliation Glaucoma versus POAG and Healthy Controls: An OCTA Study. Asia Pac J Ophthalmol (Phila) 2018;7:84-9.
50. Park JH, Yoo C, Girard MJA, et al. Peripapillary Vessel Density in Glaucomatous Eyes: Comparison between Pseudoexfoliation Glaucoma and Primary Open-angle Glaucoma. J Glaucoma 2018 (In Press).
51. Yarmohammadi A, Zangwill LM, Diniz-Filho A, et al. Peripapillary and Macular Vessel Density in Patients with Glaucoma and Single-Hemifield Visual Field Defect. Ophthalmology 2017;124:709-19.
52. Pradhan ZS, Dixit S, Sreenivasaiah S, et

al. A Sectoral Analysis of Vessel Density Measurements in Perimetrically Intact Regions of Glaucomatous Eyes: An Optical Coherence Tomography Angiography Study. J Glaucoma 2018;27:525-31.
53. Chen CL, Bojikian KD, Wen JC, et al. Peripapillary Retinal Nerve Fiber Layer Vascular Microcirculation in Eyes With Glaucoma and Single-Hemifield Visual Field Loss. JAMA Ophthalmol 2017;135:461-8.
54. Chihara E, Dimitrova G, Amano H, Chihara T. Discriminatory Power of Superficial Vessel Density and Prelaminar Vascular Flow Index in Eyes With Glaucoma and Ocular Hypertension and Normal Eyes. Invest Ophthalmol Vis Sci 2017;58:690-7.
55. Chen HS, Liu CH, Wu WC, et al. Optical Coherence Tomography Angiography of the Superficial Microvasculature in the Macular and Peripapillary Areas in Glaucomatous and Healthy Eyes. Invest Ophthalmol Vis Sci 2017;58:3637-45.
56. Takusagawa HL, Liu L, Ma KN, et al. Projection-Resolved Optical Coherence Tomography Angiography of Macular Retinal Circulation in Glaucoma. Ophthalmology 2017;124:1589-99.
57. Suh MH, Zangwill LM, Manalastas PI, et al. Deep Retinal Layer Microvasculature Dropout Detected by the Optical Coherence Tomography Angiography in Glaucoma. Ophthalmology 2016;123:2509-18.
58. Lee EJ, Kim TW, Lee SH, Kim JA. Underlying Microstructure of Parapapillary Deep-Layer Capillary Dropout Identified by Optical Coherence Tomography Angiography. Invest Ophthalmol Vis Sci 2017;58:1621-7.
59. Lee EJ, Lee KM, Lee SH, Kim TW. Parapapillary Choroidal Microvasculature Dropout in Glaucoma: A Comparison between Optical Coherence Tomography Angiography and Indocyanine Green Angiography. Ophthalmology 2017;124:1209-17.
60. Lee EJ, Lee SH, Kim JA, Kim TW. Parapapillary Deep-Layer Microvasculature Dropout in Glaucoma: Topographic Association With Glaucomatous Damage. Invest Ophthalmol Vis Sci 2017;58:3004-10.
61. Shin JW, Kwon J, Lee J, Kook MS. Choroidal Microvasculature Dropout is Not Associated With Myopia, But is Associated With Glaucoma. J Glaucoma 2018;27:189-96.
62. Lee EJ, Kim TW, Kim JA, Kim JA. Central Visual Field Damage and Parapapillary Choroidal Microvasculature Dropout in Primary Open-Angle Glaucoma. Ophthalmology 2018;125:588-96.
63. Park HL, Kim JW, Park CK. Choroidal Microvasculature Dropout Is Associated with Progressive Retinal Nerve Fiber Layer Thinning in Glaucoma with Disc Hemorrhage. Ophthalmology 2018;125:1003-13.
64. Rao HL, Pradhan ZS, Weinreb RN, et al. Determinants of Peripapillary and Macular Vessel Densities Measured by Optical Coherence Tomography Angiography in Normal Eyes. J Glaucoma 2017;26:491-7.
65. Suh MH, Zangwill LM, Manalastas PI, et al. Optical Coherence Tomography Angiography Vessel Density in Glaucomatous Eyes with Focal Lamina Cribrosa Defects. Ophthalmology 2016;123:2309-17.
66. Hollo G. Intrasession and Between-Visit Variability of Sector Peripapillary Angioflow Vessel Density Values Measured with the Angiovue Optical Coherence Tomograph in Different Retinal Layers in Ocular Hypertension and Glaucoma. PLoS One 2016;11:e0161631.
67. Spaide RF, Fujimoto JG, Waheed NK. Image Artifacts in Optical Coherence Tomography Angiography. Retina 2015;35:2163-80.
68. Venugopal JP, Rao HL, Weinreb RN, et al. Repeatability of vessel density measurements of optical coherence tomography angiography in normal and glaucoma eyes. Br J Ophthalmol 2018;102:352-7.
69. Camino A, Zhang M, Gao SS, et al. Evaluation of artifact reduction in optical coherence tomography angiography with real-time tracking and motion correction technology. Biomed Opt Express 2016;7:3905-15.
70. Venugopal JP, Rao HL, Weinreb RN, et al. Repeatability and comparability of peripapillary vessel density measurements of high-density and non-high-density optical coherence tomography angiography scans in normal and glaucoma eyes. Br J Ophthalmol 2018 (In Press).
71. Campbell JP, Zhang M, Hwang TS, et al. Detailed Vascular Anatomy of the Human Retina by Projection-Resolved Optical Coherence Tomography Angiography. Sci Rep 2017;7:42201.

Correspondence to:
Dr. Harsha Rao
Narayana Nethralaya,
Bengaluru, India